

## Supporting Information

# Tunable Surface Plasmon Polaritons and Ultrafast Dynamics in 2D Nanohole Arrays

*Min Gao,<sup>a</sup> Yonglin He,<sup>a</sup> Ying Chen,<sup>b</sup> Tien-Mo Shih,<sup>c</sup> Weimin Yang,<sup>a</sup> Jingyu Wang,<sup>a</sup> Feng Zhao,<sup>a</sup>  
Ming-De Li,<sup>\*d</sup> Huanyang Chen,<sup>b</sup> and Zhilin Yang<sup>\*a</sup>*

<sup>a</sup>Department of Physics, Collaborative Innovation Center for Optoelectronic Semiconductors and  
Efficient Devices, Xiamen University, Xiamen, 361005, China

<sup>b</sup>Institute of Electromagnetics and Acoustics and Key Laboratory of Electromagnetic Wave  
Science and Detection Technology, Xiamen University, Xiamen, 361005, China

<sup>c</sup>Department of Mechanical Engineering, University of California, Berkeley, Ca. 94720, USA

<sup>d</sup>Department of Chemistry and Key Laboratory for Preparation and Application of Ordered  
Structural Materials of Guangdong Province, Shantou University, Shantou, 515063, China

**Content:**

**S1. Sample fabrication**

**S2. Large-area SEM image**

**S3. AFM image**

**S4. Simulations in the range of 350 ~ 450 nm**

**S5. Ultrafast maps of all azimuthal angles**

**S6. Spectral shifts around plasmon dips**

**S7. Fit of figure 3 with dynamics**

**S8. Power-dependent transient  $\Delta OD$  spectra**

**S9. Phase matching equation and band gap**

**S10. Contour map of figure 4b**

**S11. Field profiles under TM polarization**

**S1. Sample fabrication:** Nanoimprint lithography (NIL) utilized in this work mainly comprises two processes: thermal NIL and UV NIL. A transparent polymer stamp (from Obducat AB, Sweden) is used for duplicating the nanostructure from the nickel master mold by thermal NIL. Then, a 2-inch silicon wafer spin-coated by a UV curable resist (Tu2-170, from Obducat AB) of about 210 nm is covered by the polymer stamp and processed at 65°C with a pressure of 30 bar for 1 min under UV exposure. Afterwards, a 2 nm adhesive layer of chromium is deposited on the substrate prior to a gold layer of about 100 nm using electron-beam evaporation (see ref. [1] for fabrication details)

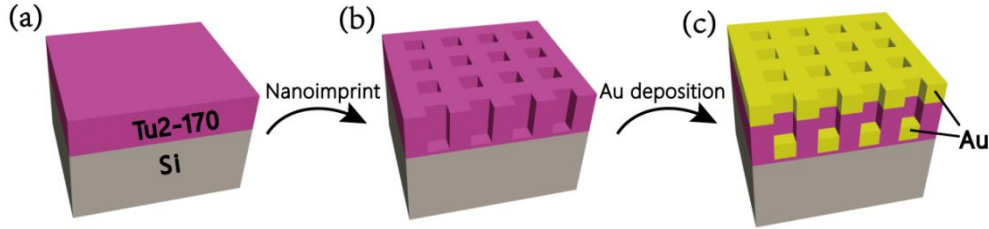


Figure S1. Sample fabrication processes

**S2. Large-area SEM image:** The image show that the 2D plasmonic arrays have uniform periodic nanostructures in a large area.

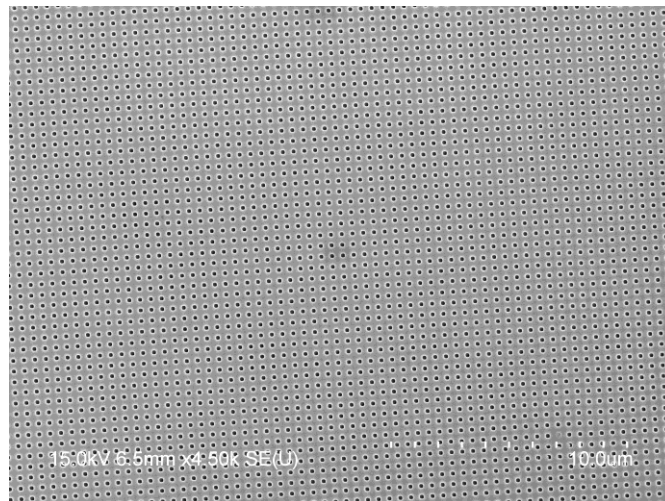


Figure S2. The SEM image in a large area.

**S3. AFM image:** The AFM image shows the depth profile. Extracting from the black dashed line after surface analysis, we can obtain the depth of the hole is  $\sim 180$  nm.

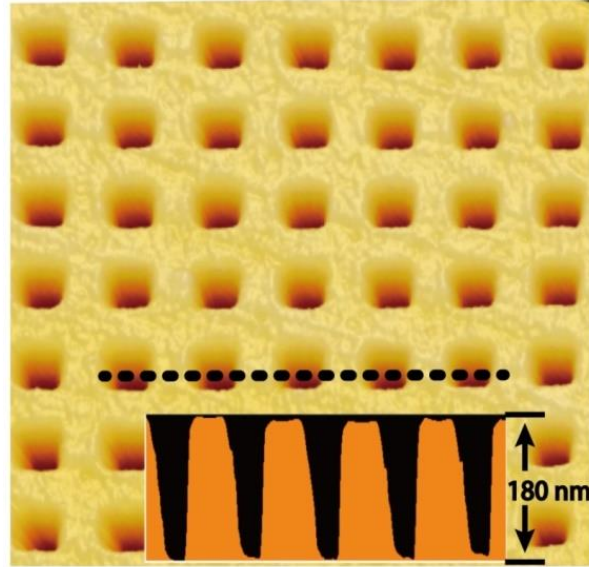


Figure S3. AFM image of the array.

**S4. Simulations in the range of 350 ~ 450 nm**

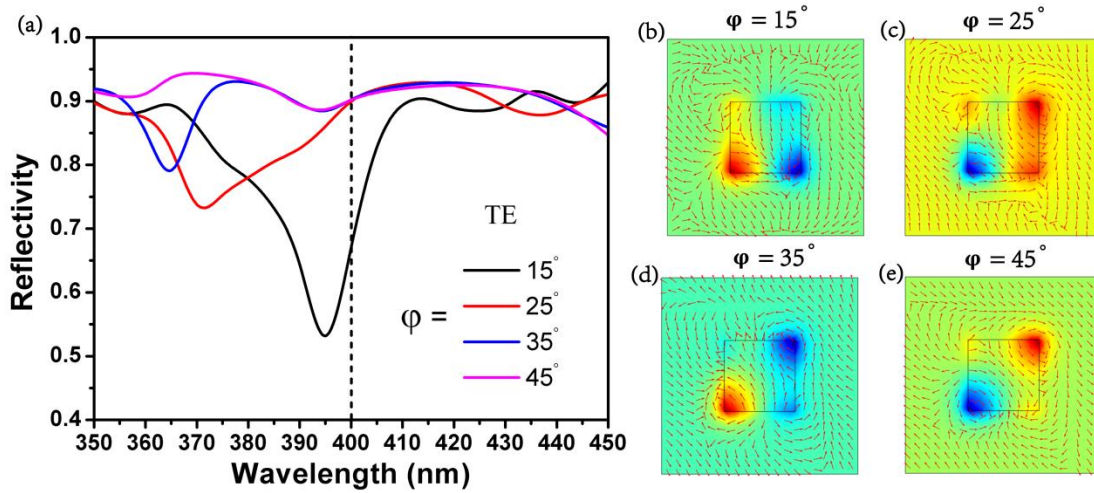
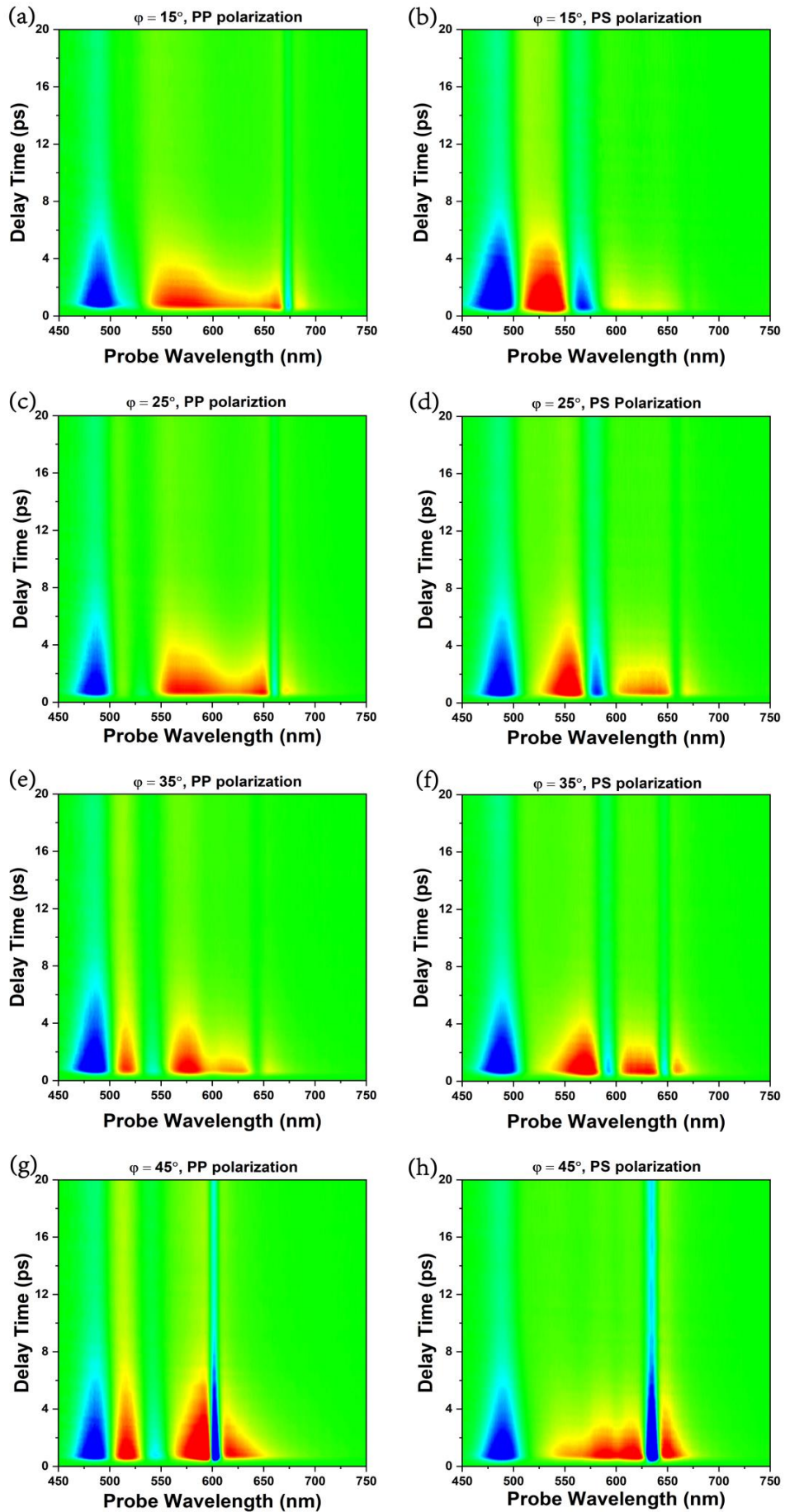


Figure S4. (a) The simulated reflectance spectra with azimuthal angles of  $15^\circ \sim 45^\circ$  in the wavelength range of 350 ~ 450 nm under TE polarization, and (b-e) corresponding electromagnetic field profile of a single nanohole cell at the wavelength of 400 nm.

**S5. Ultrafast maps of all azimuthal angles**



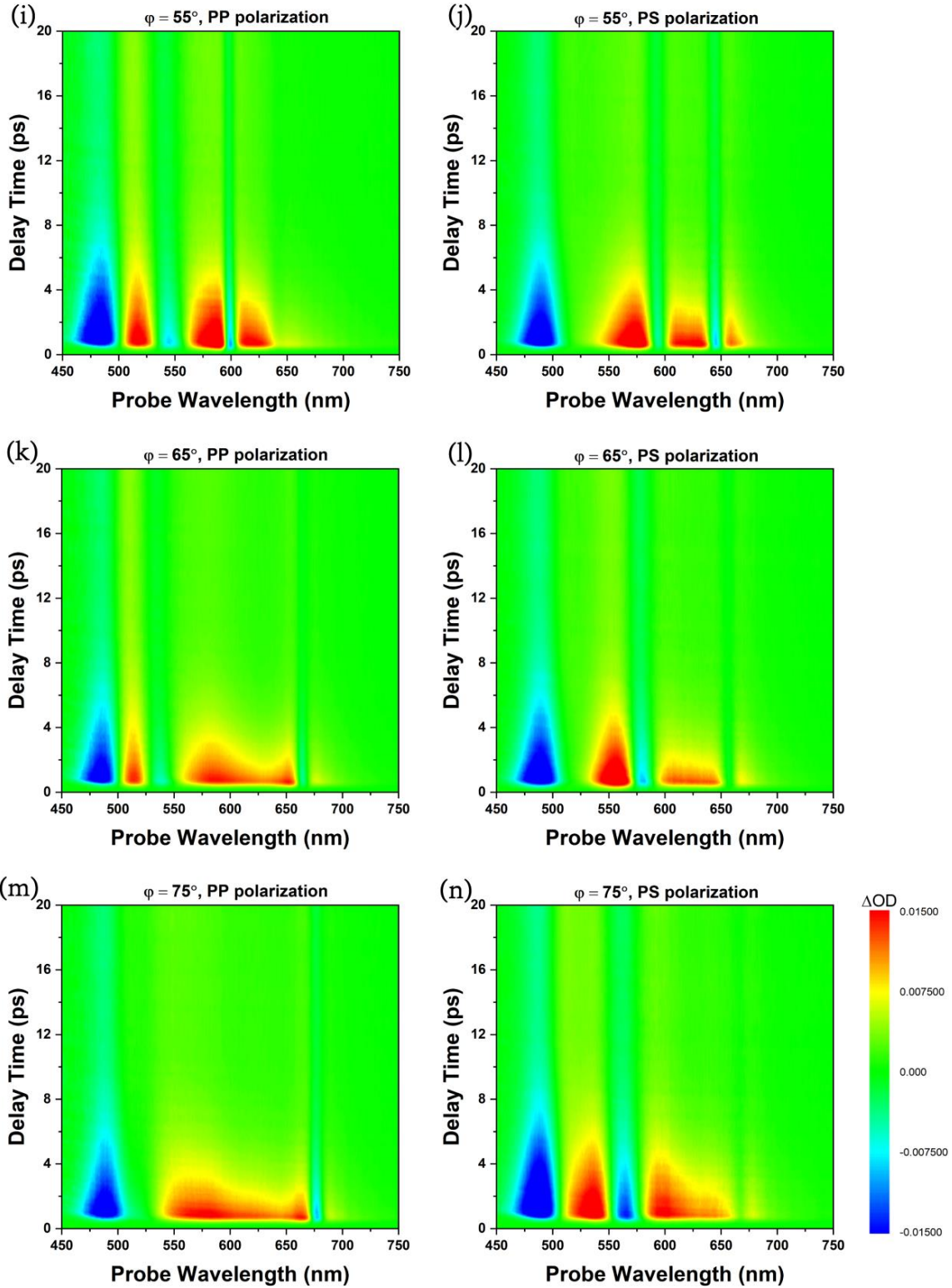


Figure S5. The  $\Delta OD$  maps at all azimuthal angles

## S6. Spectral shifts around plasmon dips

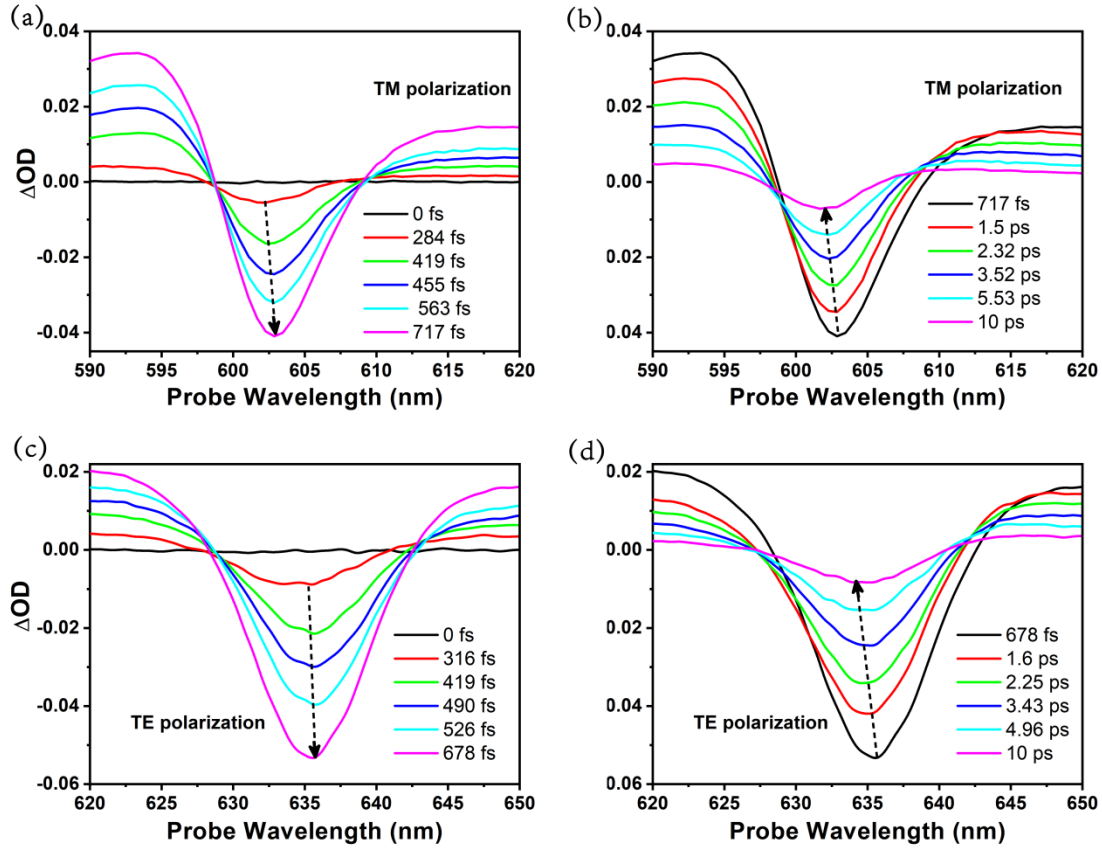


Figure S6. Enlarge Fig. 3 around the most intense plasmon dips. The black dashed lines guide the trends. Until  $\sim 700$  fs, the spectra continue to broaden and redshift, and then to narrow and shift back.

## S7. Fit of Figure 3 with dynamics

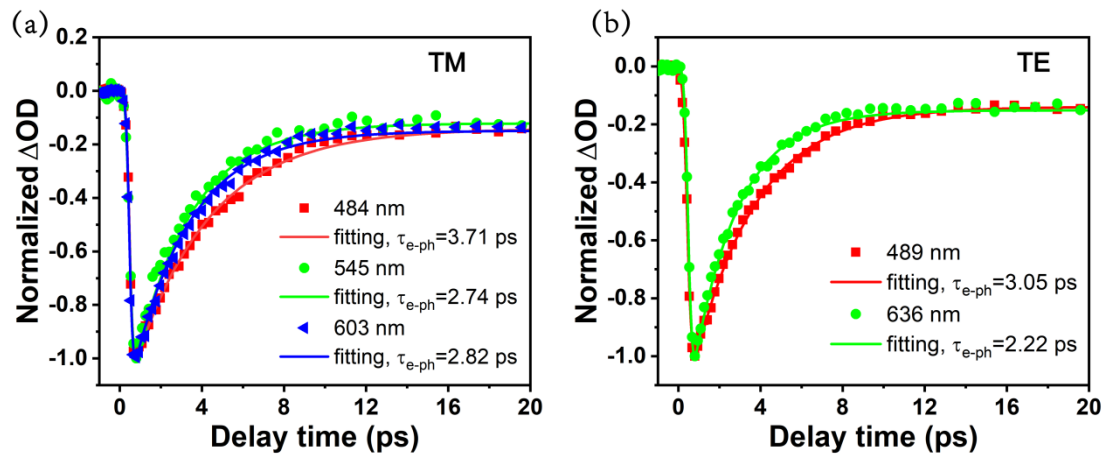


Figure S7. The corresponding time dynamics fitting of Figure 3 by a biexponential decay functions

## S8. Power-dependent transient $\Delta OD$ spectra

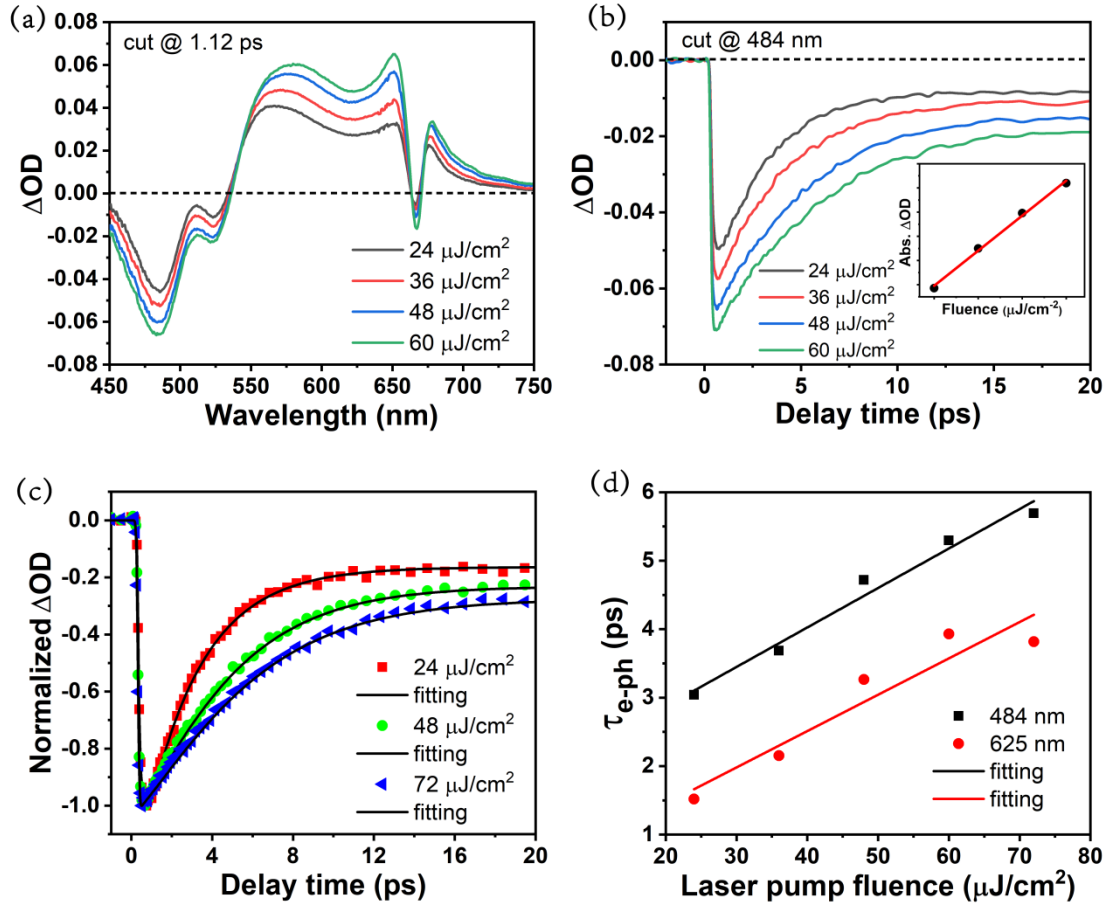


Figure S8. (a) Fluence-dependent transient  $\Delta OD$  spectra around  $20^\circ$  azimuthal angle at the delay time of 1.12 ps. (b) Fluence-dependent  $\Delta OD$  kinetics at the wavelength of 484 nm. Inset: Absolute  $\Delta OD$  versus the pump fluence. (c) Fluence-dependent normalized  $\Delta OD$  kinetics for three specific fluences of 24, 48, 72  $\mu\text{J}/\text{cm}^2$ . (d) A plot of the electron-phonon relaxation times against the pump fluence.

## S9. Phase matching equation and band gap

The dispersion relation of surface plasmon at a dielectric-metal interface can be written as

$$K_{sp} = \frac{\omega}{c} \sqrt{\frac{\epsilon_d \epsilon_m}{\epsilon_d + \epsilon_m}}. \quad (1)$$

The x-component of the wave vector can be described as

$$K_x = K \sin \theta \sin \varphi + m(2\pi/d), \quad (2)$$

and the y-component of the wave vector can be described as

$$K_y = K \sin \theta \cos \varphi + n(2\pi/d), \quad (3)$$

Where m and n denote the integer representing the diffraction order (m, n = ±1, ±2, ..).

The conservation of energy and momentum can be achieved simultaneously if the surface plasmon wave vector in Eq. (1) equals the wave vector of the incident light on the metal surface,

$$K_{sp} = (K_x^2 + K_y^2)^{1/2}. \quad (4)$$

Combining the above relations, we can obtain the phase matching equation,

$$\frac{2\pi}{\lambda_{SPP}} \sqrt{\frac{\epsilon_{Au}}{\epsilon_{Au} + 1}} = \sqrt{\left(\frac{2\pi}{\lambda_{SPP}} \sin \theta \sin \varphi + m \frac{2\pi}{P}\right)^2 + \left(\frac{2\pi}{\lambda_{SPP}} \sin \theta \cos \varphi + n \frac{2\pi}{P}\right)^2}.$$

Corresponding curves are shown below by using related MATLAB programs [2] ( $\theta$  set to 23°).

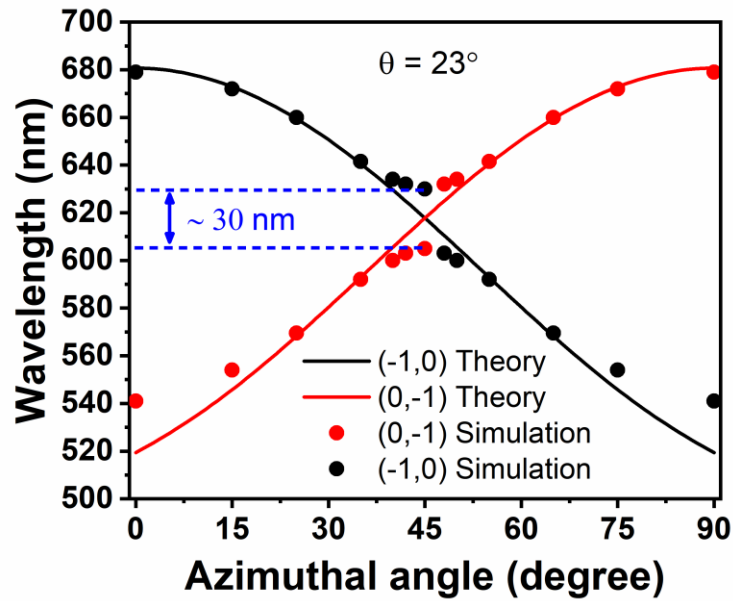


Figure S9. Theoretical curves of phase matching equation and the spectral positions of simulated SPP modes. The spectral positions of simulated (0,-1) mode (black solid circles) and (-1, 0) mode (red solid circles) as a function of the azimuthal angles. The blue double arrow indicates the plasmonic band gap of  $\sim 30$  nm.

### S10. Contour map of Figure 4b

According to the phase-matching equation, two  $(0, -1)$  and  $(-1, 0)$  SPP modes shift monotonically from  $\varphi = 0^\circ$  to  $\varphi = 90^\circ$ . For example,  $(0, -1)$  SPP mode continues the redshift from  $\varphi = 0^\circ$  to  $\varphi = 90^\circ$  (Fig. S10a), instead of first proceeding with the redshift and then turning towards the blueshift after  $\varphi = 45^\circ$  (Fig. S10b).

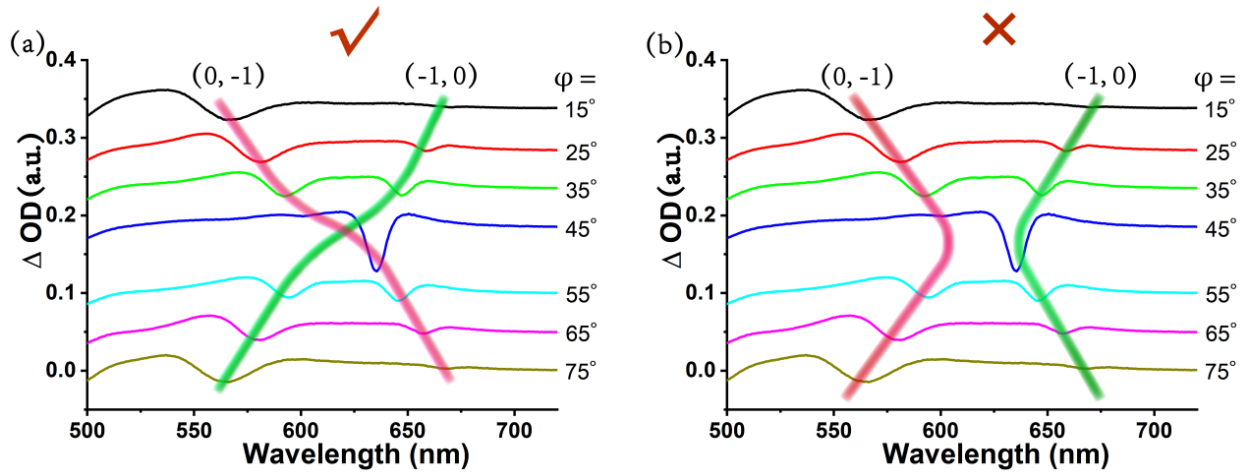


Figure S10. Illustration of modes evolution represented by contour map for Figure 4b.

## S11. Field profiles under TM polarization

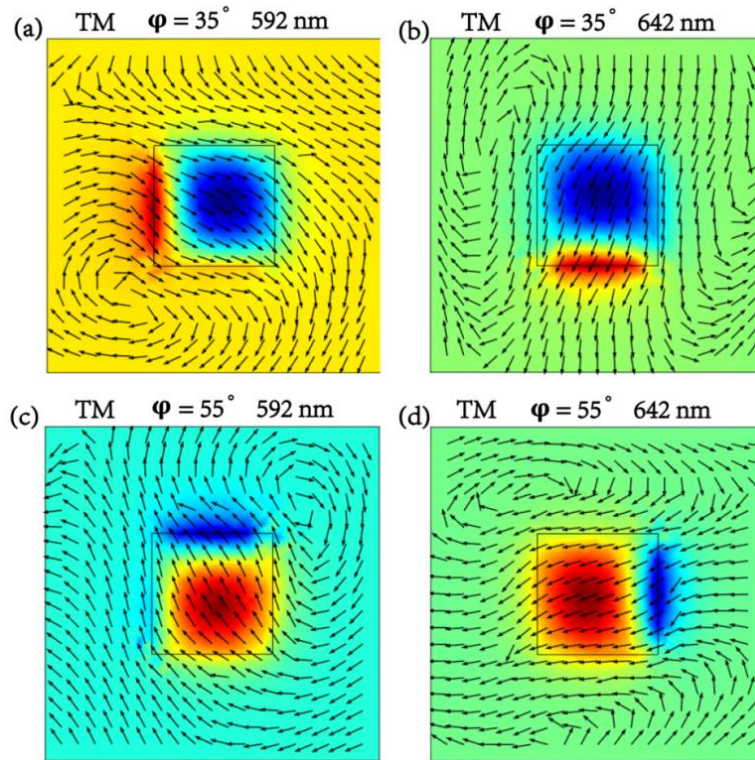


Figure S11. Electric field pattern of  $E_z$  and magnetic field vector distribution of  $H_x$ ,  $H_y$  under TM polarization. The azimuthal angles are  $35^\circ$  and  $55^\circ$  in (a, b) and (c, d), respectively. Note that: All intensities are normalized by the same scale bar.

## REFERENCES

1. J. Zhu, L. Zhang, Y. Bai, H. Liu, N. Feng, J. Zhou, B. Zeng, T. Lin, and Q. H. Liu, "Simultaneous Fabrication of Two Kinds of Plasmonic Crystals by One Nanoimprint Mold," *IEEE Photon. Technol. Lett.* **29**, 504-506 (2017).
2. B. Ung and Y. L. Sheng, "Interference of surface waves in a metallic nanoslit," *Opt. Express* **15**, 1182-1190 (2007).